Mode Scattering by a Nonlinear Step-Discontinuity in Dielectric Optical Waveguides

Samir J. Al-Bader and Hussain A. Jamid

Abstract— **The scatter of an incident TE_0 mode at a step-discontinuity separating linear and nonlinear waveguides is studied. Under certain conditions the self-focusing nonlinearity is shown to strongly modify the scattered field in comparison with the linear counterpart. The stronger effects are shown to occur when the nonlinear waveguide is operated in the cut-off condition at low power while supporting a nonlinear guided mode at high power. The method of lines is used in modeling the structure.**

I. Introduction

ONE OF the important problems in dielectric waveguides is the accurate description of the field around regions of abrupt longitudinal changes. Such changes occur in numerous practical situations, often as deliberate design features. They can be effected by variation in the geometry of the structure, or its material properties, or both. Examples of such discontinuities are encountered in cascaded waveguide sections, waveguide junctions, gratings, stepped transitions, and dielectric coatings. In integrated optics, the waveguides are, in the majority of cases, of the open type. The description of the electromagnetic field scattered by discontinuities must, therefore, involve the discrete modes and also the continuum of radiation modes. The general procedure for determining the reflection, radiation, and transmission characteristics of the discontinuity in planar structures has been to write the field components on either side of the discontinuity as a sum of discrete modes and an integral of radiation modes, and then to follow one of many approaches to assure the continuity of the tangential components on the plane of discontinuity [1]–[11]. Solutions are obtained when certain error criteria are satisfied. However, such formalism remains valid for linear structures only and is not immediately applicable, in principle, to situations in which a nonlinear feature of the structure is involved. It is the purpose of this work to study the nonlinear reflection, radiation, and transmission of the guided mode in a linear-to-nonlinear waveguide cascade.

The last decade has witnessed a rapid increase in interest in nonlinear optical guided waves. Thin film technology lends itself well to the fabrication of waveguide components in which, by virtue of the small dimensions, high power densities are obtained from relatively low power sources. Nonlinear interactions of sufficient magnitude can thus result, giving rise to important novel signal processing operations. Of interest to the present work is the nonlinear effect resulting from the dependence of the dielectric function on the field intensity of waves of one frequency. For an outlook on recent developments the reader is referred to [12]. One notes that many properties of nonlinear guided waves in planar multilayer structures, as well as their potential applications, have been reported and questions relating to their stability investigated. It has become clear that, for device implementation, materials with large nonlinear coefficients, small loss and fast response are required for the proper operation of the isolated device. Other requirements will also have to be met for the operation of devices in a system and these are likely to be system-specific. It turns out, nevertheless, that the above material requirements are often not concurrently available in important waveguide materials and trade-offs have to be made as, for example, between the amount of the intensity-induced refractive index change and the total loss. The currently considered materials with potential third-order nonlinear applications to high speed communication systems include polymers, glasses, and semiconductors.

The power-dependent transmission of nonlinear waveguides has been discussed in the past for various longitudinally uniform and nonuniform waveguide configurations [13]–[15]. To our knowledge, no rigorous analysis of the mode scatter problem has been given. The transmission of optical power above a certain threshold in nonlinear waveguides has been demonstrated theoretically [14]. The power-dependent transmission in a linear-nonlinear-linear waveguide cascade has been observed experimentally. Waves launched in a linear film have been made to traverse a small nonlinear section with liquid crystal MBBA as its upper cladding material [16]. A drop in the transmitted power with increasing incident power has been observed in this experiment. In [17], a waveguide made of 0.7 μm silicon film on sapphire has been used to experimentally demonstrate the intensity-induced switching of the guided mode excitation. Utilizing a grating coupler and operating at photon energies near the bandgap, fast switching due to electronic and thermal nonlinearities has been observed to occur with increasing power.

There are two motivations for the present work. The first is to investigate the inevitable occurrence, in nonlinear circuits where the signal is serially processed, junctions of waveguides of different types (linear and nonlinear). It is important for

Manuscript received November 17, 1994; revised November 12, 1995. This work was supported by King Fahd University of Petroleum and Minerals.

The authors are with King Fahd University of Petroleum and Minerals, Dhahran, Saudi Arabia.

Publisher Item Identifier S 0018-9480(96)01446-9.

this reason to study the nonlinear reflection, transmission, and radiation properties of guided modes and also to establish analysis techniques suited for their description.

The second motivation is to examine the introduction of longitudinal discontinuities for the potential enhancement of the effects of nonlinearities. In the present work we study the scatter of the TE_0 guided mode supported by a linear (input) waveguide at the junction with an (output) nonlinear one. A sudden reduction in the width of the nonlinear core of the latter waveguide or a depression in its index causes it to be cut-off at low power with the transmitted field being radiative in character. The nonlinear core is taken to be self-focusing, so that with increasing input power the output waveguide can be made to support the nonlinear TE_0 mode. It will be shown that both the onset of the change from radiative to guided field as well as the difference in the available power at a distance of one millimeter from the junction are influenced by the step discontinuity and also by the magnitude of the nonlinearity. We use the method of lines [18], [19] in our analysis and make no assumptions on the magnitude of the step-change or the nonlinearity. Formulation of the method of solution is given in Section III. The results of Section IV show that the method, used within the self-consistent scheme described in Section III, is suited to the determination of the various aspects of the nonlinear field.

II. Theory

Fig. 1 gives a schematic representation of the structure of interest. The plane $z = 0$ separates the linear input dielectric waveguide ($z < 0$) from the nonlinear output one ($z > 0$). All regions shown in the figure, except that of the core of the nonlinear waveguide, are assumed to be linear. The core of the nonlinear waveguide is taken to be nonlinear with its dielectric function having a saturable self-focusing nonlinearity. The dielectric function of the core region of the complete structure is written as,

$$\begin{aligned} \varepsilon_2 &= \varepsilon_b & z < 0 \\ \varepsilon_2 &= \varepsilon_b + \Delta\varepsilon\left(1 - e^{-|E|^2}\right) & z > 0 \end{aligned} \tag{1}$$

where $\varepsilon_b = n_b^2$ and n_b is the refractive index of the core region at low power. The superstrate and substrate have indices given by n_1 and n_3, respectively. Our interest is to determine the spatial distribution of the field throughout the structure when the TE_0 mode is assumed to be incident from the left onto the plane of discontinuity. The core of the nonlinear waveguide is made to undergo a sudden reduction in width or depression in index of sufficient magnitude as to render it to be cut off to the incident mode at low power.

The effects we study arise as a result of allowing the power of the incident mode to increase sufficiently so that the nonlinear TE_0 mode is supported at the output end of the nonlinear waveguide. The saturable form of nonlinearity given by the second of (1), while suppressing the scaling factor, assumes that the electric field intensity $|E|^2$ is scaled as has been discussed in [20]. The nonlinear response of different materials is thus accounted for through the scaled field. Referring to the coordinate system shown in Fig. 1 the

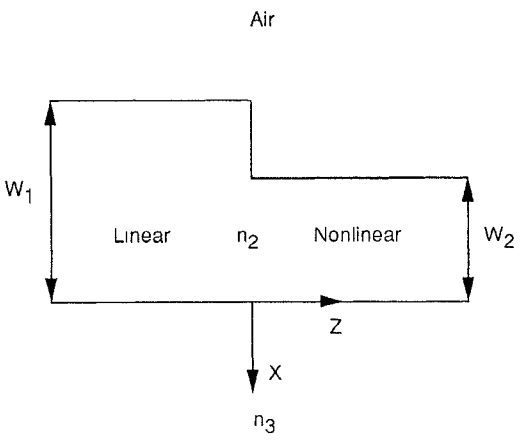

Fig. 1. Schematic diagram of the structure studied. The TE_0 mode is assumed to be incident from the left at the discontinuity plane $z = 0$. The parameters used throughout the work are $\varepsilon_1 = 1$, $\varepsilon_b = 2.3104$, $\varepsilon_3 = 2.25$, $\lambda = 1.55$ μm and $W_1 = 4$ μm.

field components of the TE_0 mode are: H_x, E_y, and H_z. For simplicity of notation we make $E_y = \psi$ and write the Helmholtz equation with the time harmonic variation $e^{-i\omega t}$ as

$$\frac{\partial^2\psi}{\partial x^2} + \frac{\partial^2\psi}{\partial z^2} + k_0^2\varepsilon_n\psi = 0 \tag{2}$$

where k_0 is the free space wave number and ε_n is the dielectric constant of any of the regions depicted in Fig. 1.

In the following, we give a formal description of the application of the method of lines [19] to (2) without making a specific reference to either the linear or the nonlinear waveguides. We also indicate that third-order absorbing boundary conditions have been incorporated in the calculations of Section III but are not given in this section. The first step is to reduce the dimensionality of (2) by replacing the variable ψ in the x-direction by the vector of discrete values, $\bar{\psi} = [\psi_1, \psi_2, \cdots, \psi_N]^t$ and also by replacing the first term on the left-hand side of (2) by its central differences approximation. It is noted that the symbol t here stands for transpose and should not be confused with the symbol for time. In the approximation made above, the points $1, 2, \cdots, N$, marked on the x-axis, enclose the whole width of the structure of interest. Equation (2) thus becomes

$$\frac{d^2\bar{\psi}}{dz^2} + \bar{Q}^2\bar{\psi} = 0 \tag{3}$$

where

$$\bar{Q}^2 = \frac{1}{(\Delta x)^2}\begin{bmatrix} -2 & 1 & 0 & 0 & 0 \\ 1 & -2 & 1 & 0 & 0 \\ 0 & 1 & -2 & 1 & 0 \\ \cdot & \cdot & \cdot & \cdot & \cdot \\ \cdot & \cdot & 0 & 1 & -2 \end{bmatrix} + k_0^2\begin{bmatrix} \varepsilon_1 & 0 & 0 & 0 & 0 \\ 0 & \varepsilon_2 & 0 & 0 & 0 \\ \cdot & \cdot & \cdot & \cdot & \cdot \\ \cdot & \cdot & \cdot & \cdot & \cdot \\ 0 & 0 & 0 & 0 & \varepsilon_N \end{bmatrix} \tag{4}$$

where $\varepsilon_1, \varepsilon_2, \cdots, \varepsilon_N$ are local dielectric constant values read at the transverse locations of $\psi_1, \psi_2, \cdots, \psi_N$ and Δx is the

discretization interval in the x-direction. The formal solution of (3) is

$$\bar{\psi}(z) = e^{\imath\bar{Q}z}\bar{a} + e^{-\imath\bar{Q}z}\bar{b}. \tag{5}$$

The first term on the right-hand side represents forward-going waves while the second term represents backward-going waves. The vector quantities $\bar{a}$ and $\bar{b}$ are, respectively, the forward and backward values of $\bar{\psi}$ at $z = 0$. The calculation of the exponentials in (5) is effected through diagonalizing the matrix $\bar{Q}^2$ such that

$$\bar{Q}^2 = \bar{T}\bar{\beta}^2\bar{T}^{-1} \tag{6}$$

where $\bar{T}$ is a square matrix whose columns are the eigenvectors of $\bar{Q}^2$ while $\bar{\beta}^2$ is a diagonal matrix whose diagonal elements are the eigenvalues of $\bar{Q}^2$. It follows that,

$$\bar{Q} = \bar{T}\bar{\beta}\bar{T}^{-1} \tag{7}$$

and

$$e^{\pm\imath\bar{Q}z} = \bar{T}e^{\pm\imath\bar{\beta}z}\bar{T}^{-1}. \tag{8}$$

Making reference to the structure of Fig. 1, there are two sets of solutions of the type given in (5), one for each of the two longitudinally uniform regions. Accordingly, the field for the whole structure can be written as

$$\bar{\psi}_{\mathrm{I,II}} = e^{\imath\bar{Q}_{\mathrm{I,II}}z}\bar{a}_{\mathrm{I,II}} + e^{\imath\bar{Q}_{\mathrm{I,II}}z}\bar{b}_{\mathrm{I,II}} \tag{9}$$

where the subscripts I and II refer to region I ($z < 0$) and region II ($z > 0$), respectively. We note that the reflected field in the region $z > 0$ is zero ($\bar{b}_{\mathrm{II}} = 0$). Continuity of the tangential field components at the plane $z = 0$ allows us to write the relationship between the transmitted and the incident fields at this position as

$$\bar{a}_{\mathrm{II}} = (\bar{Q}_{\mathrm{I}} + \bar{Q}_{\mathrm{II}})^{-1}(2\bar{Q}_{\mathrm{I}})\bar{a}_{\mathrm{I}}. \tag{10}$$

The presence of the nonlinearity in the region $z > 0$ requires special attention in order that the action of the field on the nonlinear core is accounted for in accordance with (1). To achieve this and, hence, to assure the continuity of the tangential field components across the plane $z = 0$, calculations are made iteratively and the dielectric function of the nonlinear core calculated each time at all points within the core according to the second of (1). In each iteration, therefore, one obtains a graded-index distribution within the nonlinear core and a corresponding set of amplitude vectors $\bar{a}_{\mathrm{I}}, \bar{b}_{\mathrm{I}}$, and $\bar{a}_{\mathrm{II}}$. The procedure is started by exciting the structure with the pre-determined TE_0 mode of the linear waveguide and initially overlooking the nonlinear term in the second of (1). It is then repeated until self-consistent conditions are obtained. Excellent convergence has been obtained after four or five iterations.

III. Results and Discussion

As a consequence of the nonlinearity in the core of the output waveguide, all of the important parameters in the description of the structure of Fig. 1, such as the reflectivity and transmissivity of the mode as well as the radiation field, are nonlinear. It is necessary, from the outset, to determine the power-dependent stationary mode behavior of the output waveguide when isolated from the input one. Although both the propagation wave vector and the field profile become power-dependent in the nonlinear waveguide, the important relationship in the present case is that between the propagation constant (or mode index) of the nonlinear TE_0 mode and the power carried by it. In order to obtain this relationship (also referred to as the dispersion relationship) the mode is assumed to vary with distance as $e^{\imath\beta z}$ where the propagation constant β is related to the mode index by $\beta = k_0 n_e$. In obtaining the dispersion curves of the nonlinear TE_0 mode we have followed the method of solution described by us in [20] and the interested reader is referred to this reference. In the following we give results on two types of discontinuity, one resulting from a change in width of the core of the output waveguide and the other from a change in its index of refraction.

A. The Geometric Step-Discontinuity

The parameters we have used in this subsection are: $\varepsilon_1 = 1$, $\varepsilon_b = 2.3104$, $\varepsilon_3 = 2.25$, $W_1 = 4\ \mu$m, and $\lambda = 1.55\ \mu$m. Several values of W_2 and $\Delta\varepsilon$ have been considered. Fig. 2 shows the dispersion curves for the following values of W_2: $1.2\ \mu$m, $1.35\ \mu$m, $2\ \mu$m and $4\ \mu$m. All curves correspond to $\Delta\varepsilon = 0.06$. It is noted that the waveguide with $W_2 = 1.2\ \mu$m (broken curve) is below cut-off for the TE_0 mode at low input power, while that with $W_2 = 1.35\ \mu$m (solid curve) is near cut-off. The rise in mode power observed near the origin for $W_2 = 1.2\ \mu$m is a well-known feature of the nonlinear TE_0 mode dispersion when this mode is below cut-off at low power. Modes falling on this branch have been shown to be unstable with increasing propagation distance and are not excited in the present work. The absence of the unstable branch in the rest of the curves of Fig. 2 is due to the fact that they correspond to waveguides that are near or above cut-off at low power. When the incident mode in the input arm of the structure of Fig. 1 gives rise to a nonlinear guided mode (beyond a certain transient distance from the step) the mode-index and mode-power values of the latter define a point on the dispersion curve. Two such points marked A and B are shown in Fig. 2 for $W_2 = 1.2\ \mu$m. They have been obtained by step-marching the field according to the algorithm described below for a sufficiently long distance for it to reach the steady state. The points are also shown in Fig. 3.

Referring to Fig. 2, points A and B, as calculated by the step-marching algorithm, are seen to exhibit good agreement with the dispersion curve. Any differences that exist are due to the fact that the dispersion curves are obtained by solving the eigenvalue equation for stationary nonlinear modes rather than by step-marching the field. It is noted that whereas point A corresponds to a well-guided mode, point B corresponds to a mode that is near cut-off. For the wider core waveguides $W_2 = 2\ \mu$m and $W_2 = 4\ \mu$m, the TE_0 mode is supported at low power. Each of the two curves for these widths starts from the linear value of n_e and exhibits near proportionality between mode index and mode power for the range shown.

The action of the nonlinear step discontinuity may be summarized as follows: a proportion of the incident mode power is transmitted beyond the plane of the step with the

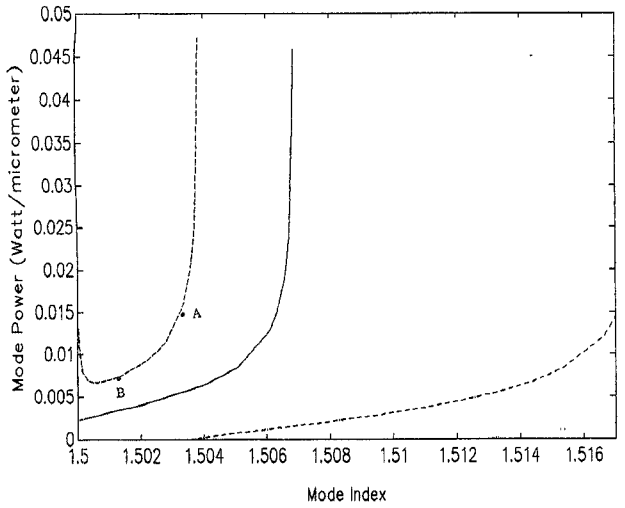

Fig. 2. Dispersion curves of the fundamental mode of the nonlinear (output) waveguide for $\Delta\varepsilon = 0.06$. $W_2 = 1.2$ μm (broken curve), $W_2 = 1.35$ μm (solid curve), $W_2 = 2$ μm (dash-dot curve), and $W_2 = 4$ μm (dotted curve).

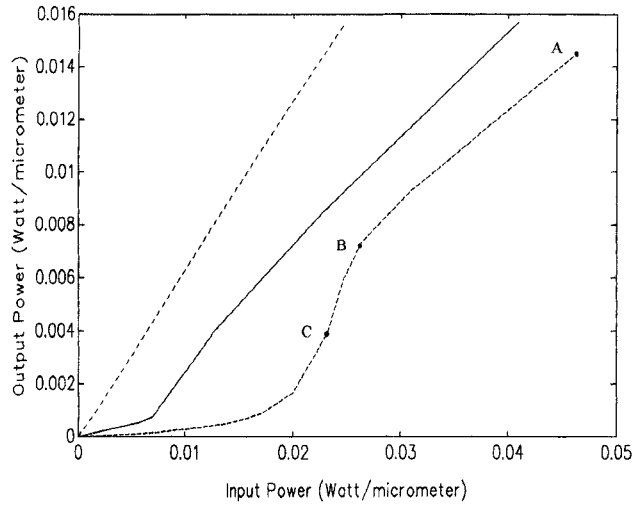

Fig. 3. The input power-output power relationship of the structure for $\Delta\varepsilon = 0.06$. Points A and B are also shown in Fig. 2. The transition from radiative to guided output is seen to occur with increasing input power. $W_2 = 1.2$ μm (broken curve), $W_2 = 1.35$ μm (solid curve), $W_2 = 2$ μm (dash-dot curve) and $W_2 = 4$ μm (dotted curve). Output power for $W_2 = 0.6$ μm is of order 10^{-5} throughout.

balance of power being reflected (small for all cases considered in this work). Of the transmitted power a proportion may evolve into a stable nonlinear mode—otherwise the whole of the transmitted power will radiate outwards. The parameters that determine the outcome of this process are $W_2, \Delta\varepsilon$, and the incident power. It is noted that for a given value of $\Delta\varepsilon$ there corresponds a minimum value of W_2 below which the linear mode will not be excited, i.e., the output waveguide remains cutoff for all incident power levels. This is due to the fact that we have adopted in this work a saturable nonlinearity according to which the maximum change in the dielectric constant ε_2 is limited to $\Delta\varepsilon$. For $\Delta\varepsilon = 0.06$ the lowest value of W_2 to support the nonlinear TE_0 mode is approximately 0.9 μm. As W_2 is increased toward W_1 the nonlinear guided mode becomes supported and the structure transforms the linear input into a nonlinear output mode of approximately the same power.

The relationship between the linear waveguide mode power (input power) and the nonlinear power that remains in the computational window at a distance $z = 1$ mm (referred to as the output power) is shown in Fig. 3. The curves for $W_2 = 2$ μm and $W_2 = 4$ μm exhibit a linear variation of output power with input power in the range of the figure. The slopes are determined by scatter and radiation losses. More detailed variation is shown by the curves for $W_2 = 1.35$ μm and $W_2 = 1.2$ μm. It is seen that transition mid-power regions connect near linear high and low power regions. Referring to the curve for $W_2 = 1.2$ μm, the portion of the curve between points A and B shows that the nonlinear mode is supported by the output waveguide. For point B an input power of 2.63×10^{-2} W/μm has been found to give rise to an output power of 7.29×10^{-3} W/μm, while for point A the corresponding values are 4.63×10^{-2} and 14.49×10^{-3} respectively. Below point B the field in the output waveguide is radiative and the incident power is insufficient to cause the excitation of the nonlinear mode. Point C in Fig. 3 corresponds to this kind of radiative field and it is for this reason that point C does not occur on the dispersion curve of Fig. 2 for $W_2 = 1.2$ μm.

The transition between the low power and the high power portions of the curves for $W_2 = 1.35$ μm and $W_2 = 1.2$ μm will be illustrated further with the aid of Fig. 6. We have also made calculations here for a waveguide whose width is below the minimum to support a nonlinear mode. The results for $W_2 = 0.6$ μm have shown that the output power over the range of input power of Fig. 3 is of order 10^{-5} W/μm and is therefore coincidental with the horizontal axis.

Examination of the influence of the magnitude of the nonlinearity has been made for $W_2 = 1.2$ μm by calculating the input power–output power curves for the additional values of $\Delta\varepsilon = 0.04$ and $\Delta\varepsilon = 0.02$. The results are shown in Fig. 4, together with those for $\Delta\varepsilon = 0.06$. As in Fig. 3, the transition toward guided nonlinear modes is noticeable for all cases. The larger nonlinearity, however, caused faster transitions that also occurred at lower input power levels.

In order to follow the evolution of the scattered field into the nonlinear waveguide, calculations have been made of the profile of transverse electric field components at $z = 10, 50, 100, 520$, and 1000 μm and shown in Fig. 5 (a)–(c). The algorithm followed is

$$\bar{\psi}_{II}(z + \Delta z) = e^{i\bar{Q}_{II}\Delta z}\bar{\psi}_{II}(z) \tag{11}$$

where Q_{II} is calculated locally at dz intervals and one-way transmission into the nonlinear waveguide assumed. Application of this kind of procedure to nonlinear waveguides, together with a comparison with results obtained by the Beam Propagation Method are found in a recently published work [21]. This work, however, considers a longitudinally-invariant structure. It is seen from Fig. 5(a) (corresponding to point A in Figs. 2 and 3) and Fig. 5(b) (corresponding to point B) that sustained power is available at the output in the shape of a nonlinear guided mode. This is in contrast to Fig. 5(c) (corresponding to point C in Fig. 3) where the

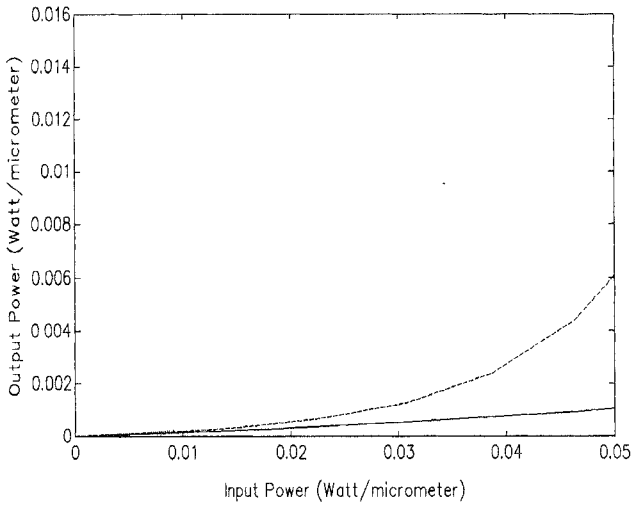

Fig 4 Input power versus output power for $W_2 = 1.2$ μm. $\Delta\varepsilon = 0.02$ (solid curve), $\Delta\varepsilon = 0.04$ (broken curve) and $\Delta\varepsilon = 0.06$ (dotted curve).

power becomes depleted in the computational window with increasing distance.

Fig. 6 shows the variation of the forward radiated power (as a ratio of input power) with the input power. Values of the forward radiated power are obtained by subtracting the output power (at 1 mm distance) from the power transmitted across the discontinuity plane. Four values of W_2 are considered with $\Delta\varepsilon = 0.06$. It is seen from the figure that almost all of the incident power for $W_2 = 0.6$ μm is forward-radiated and remains so for the whole range of input power. In the case of $W_2 = 2$ μm the proportion of the forward-radiated power shows a small initial drop from the linear value becoming almost independent of the increasing input power. In contrast to this behavior, the curves for the intermediate values of $W_2 = 1.2$ μm and $W_2 = 1.35$ μm exhibit strong variation in the forward-radiated power. At low input power the power balance is dominated by forward-radiation. With increasing input power a larger proportion of the input goes into the guided mode with the percentage of radiated power becoming approximately independent of the input power. A steep transition is noticeable in each of the two cases with approximately 30 % change in forward-radiation resulting from the self-action of the field. As might be expected, Fig. 6 indicates that the two conditions associated with the stronger changes are (a) that the output waveguide is cut-off at low power, and (b) that a nonlinear mode is supported at high power.

The percentage of backward-radiated power has been found to be small and almost independent of the input power for all values of W_2 considered, as seen from Fig. 7. Calculations for $W_2 = 4$ μm give a ratio of backward radiation/input power of order 10^{-5} throughout.

B. The Index Step-Discontinuity

When the waveguides on either side of the discontinuity are of identical dimensions strong power-dependent changes can occur when the core index of the output waveguide is sufficiently depressed that it acts as an anti-guide at low power.

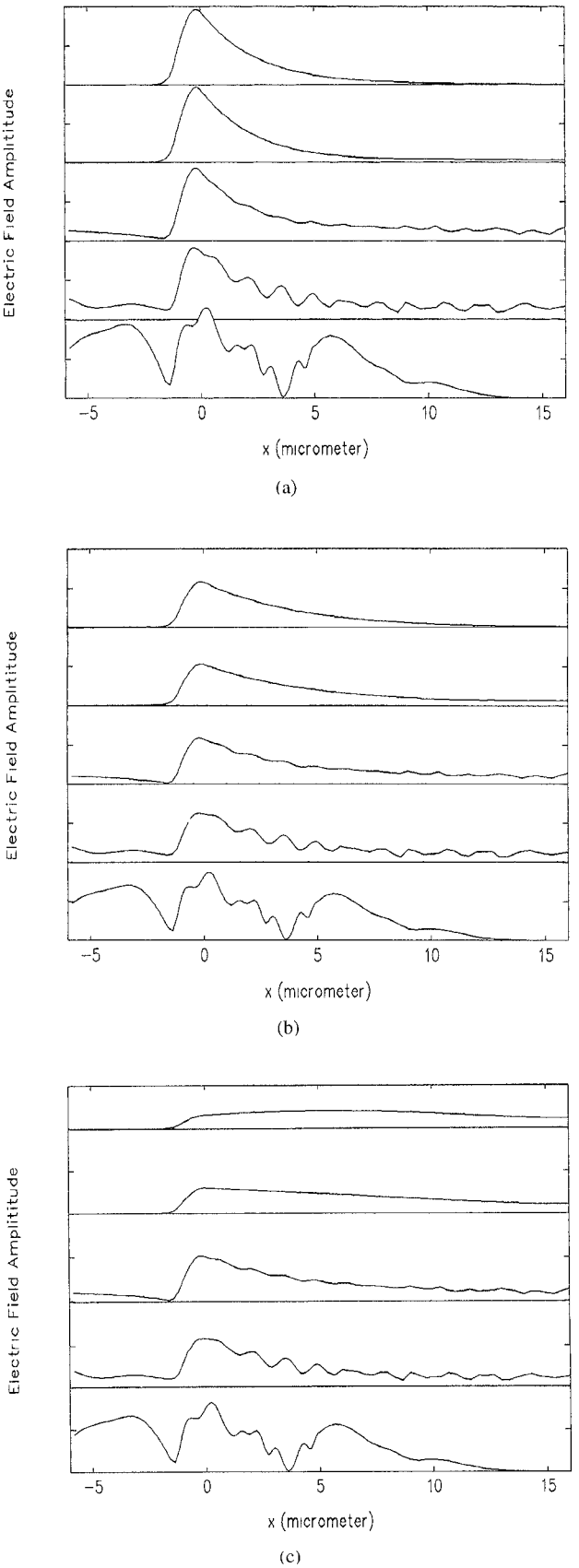

Fig. 5. (a)–(c) Profile of E_y in the nonlinear waveguide at $z = 10, 50, 100, 520$, and 1000 μm. Distances increase upwards on the vertical axis. The power associated with (a)–(c) correspond to those of point A-C of Fig. 3, respectively. The output waveguide core is 1.2 μm and $\Delta\varepsilon = 0.06$.

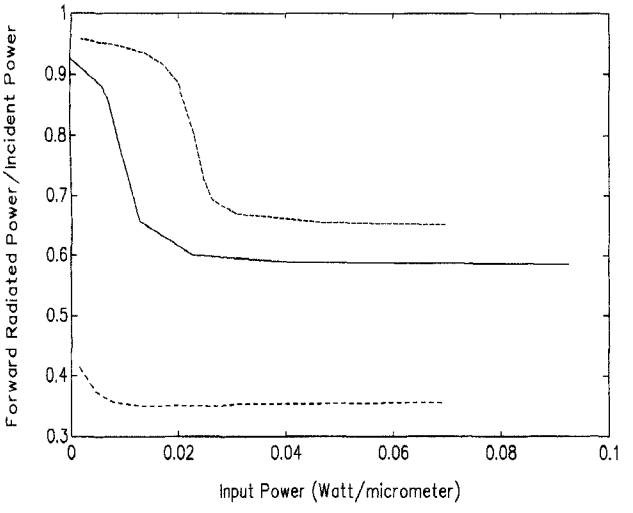

Fig. 6. Ratio of forward radiated power to the incident power as a function of the incident (input) power for $\Delta\varepsilon = 0.06$. $W_2 = 0.6$ μm (dotted curve), $W_2 = 1.2$ μm (broken curve), $W_2 = 1.35$ μm (solid curve) and $W_2 = 2$ μm (dash-dot curve). Values of forward radiated power/input power for $W_2 = 4$ μm are of order 10^{-2}.

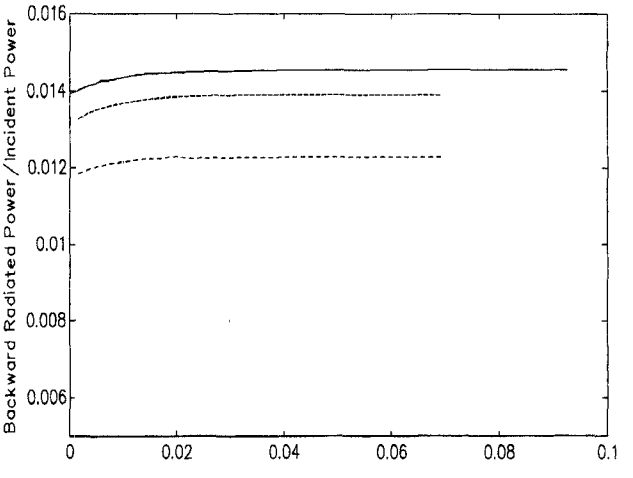

Fig. 7. Ratio of the backward radiated power to the incident power as a function of the incident power. All parameters are as in Fig. 6.

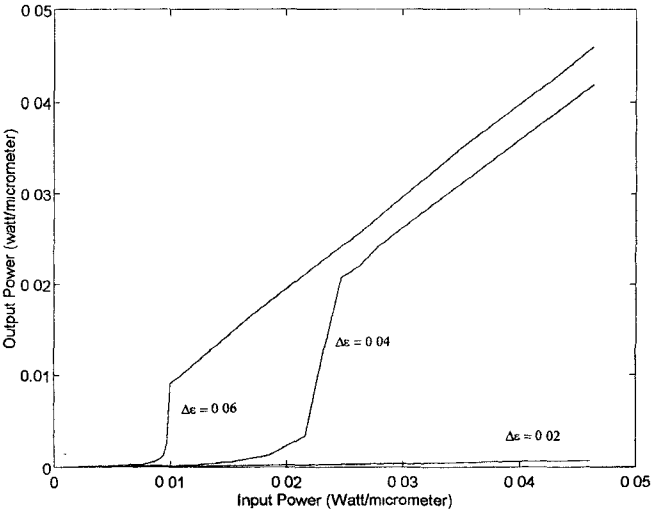

Fig. 8. The input power-output power relationship for $W_1 = W_2 = 4$ μm. The core dielectric constant $\varepsilon_b = 1.495^2 (z > 0)$. Other parameters are as in Fig. 6.

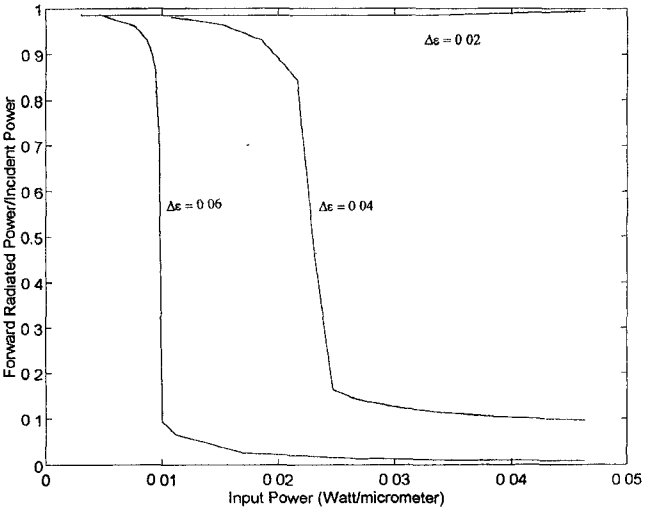

Fig. 9. Ratio of the forward radiated power to the incident power. The parameters are as in Fig. 8.

As in Section III-A, self-action of the field is necessary for the establishment of the nonlinear guided mode with increasing power. To demonstrate the fast changes that can occur in the guided and forward radiated power we have adopted $W_1 = W_2 = 4$ μm and used the value $\Delta\varepsilon = 2.235\,025$ $(z > 0)$ while retaining all the other parameters of Section III-A. Fig. 8 shows the output power variation with input power. Fast changes are seen to separate the radiative and guided field regions for $\Delta\varepsilon = 0.06$ and $\Delta\varepsilon = 0.04$.

The output power has been found to be very small for $\Delta\varepsilon = 0.02$. Fig. 9 shows the proportional change in the forward radiated power. Changes of the order of 90% are seen to occur with the stronger nonlinearity.

IV. Conclusion

The nonlinear scatter of the guided mode at the junction of linear-to-nonlinear waveguides has been studied as a function of input power by the method of lines. Both geometric and index step changes in the structure have been considered. In both cases the presence of nonlinearity is shown to modify the scattered field in comparison with linear behavior. For the geometric step-discontinuity the modification can be strong but is found to be dependent on step size. For the input power range considered, the scattered field of the smallest and largest step sizes used in the calculations is approximately that predicted by linear theory. For intermediate step sizes associated with low power cut-off conditions of the nonlinear waveguide, substantial modifications of linear results have been found to occur. Strong changes in the output field have also been found to occur when the two waveguides are of identical dimensions but differ a little in their index distributions.

References

[1] C. M. Angulo, "Diffraction of surface waves by a semi-infinite dielectric slab," *IRE Trans. Antenn. Propg.*, vol. AP-5, pp. 100–109, 1957.

[2] T. Ikegami, "Reflectivity of mode at facet and oscillation mode in double-heterostructure injection lasers," *IEEE J. Quant. Elect.*, vol. QE-8, pp. 470–476, 1972.
[3] S. Mahmoud and J. Beal, "Scattering of surface waves at a dielectric discontinuity on a planar waveguide," *IEEE Trans. Microwave Theory Tech.*, vol. MTT-23, pp. 193–198, 1975.
[4] G. H. Brook and M. Kharadly, "Step discontinuities on dielectric waveguides," *Elect. Lett.*, vol. 12, pp. 473–475, 1976.
[5] T. Rozzi, "Rigorous analysis of the step discontinuities in planar dielectric waveguides," *IEEE Trans. Microwave Theory Tech.*, vol. MTT-26, pp. 738–746, 1978.
[6] K. Morishita, S.-I. Inagaki, and N. Kumagai, "Analysis of discontinuities in dielectric waveguides by means of the least squares boundary residual method," *IEEE Trans. Microwave Theory Tech.*, vol. MTT-27, pp. 310–315, 1979.
[7] P. Gelin, S. Toutain, and J. Citerne, "Scattering of surface waves on transverse discontinuities in planar dielectric waveguides," *Radio Sci.*, vol. 16, pp. 1161–1165, 1981.
[8] P. Gelin, M. Petenzi, and J. Citerne, "Rigorous analysis of the scattering of surface waves in an abruptly ended slab dielectric waveguide," *IEEE Trans. Microwave Theory Tech.*, vol. MTT-29, 1981.
[9] G. H. Brook and M. Z. Kharadly, "Scattering by abrupt discontinuities on planar dielectric waveguides," *IEEE Trans. Microwave Theory Tech.*, vol. 30, pp. 760–770, 1982.
[10] H. Shigesawa and M. Tsuji, "Mode propagation through a step discontinuity in dielectric planar waveguide," *IEEE Trans. Microwave Theory Tech.*, vol. 34, pp. 205–212, 1986.
[11] H. Shigesawa and M. Tsuji, "A new equivalent network method for analyzing discontinuity properties of open dielectric waveguides," *IEEE Trans. Microwave Theory Tech.*, vol. 37, pp. 3–14, 1989.
[12] G. I. Stegeman and H. E. Ponath, Eds., *Nonlinear Surface Electromagnetic Phenomena*. Amsterdam: North Holland, 1991.
[13] G. R. Olbright *et al.*, "Microsecond room-temperature optical bistability and cross talk studies in ZnS and ZnSe interference filters with visible light and milliwatt power," *Appl. Phys. Lett.*, vol. 45, pp. 1031–1033, 1984.
[14] C. T. Seaton *et al.*, "Anomalous guided wave cut off phenomena," *Appl. Phys. Lett.*, vol. 45, pp. 1162–1163, 1984.
[15] L. Leine *et al.*, "Propagation phenomena of nonlinear film-guided waves: A numerical analysis," *Opt. Lett.*, vol. 11, pp. 590–592, 1986.
[16] H. Vach *et al.*, "Observation of intensity-dependent guided waves," *Opt. Lett.*, vol. 9, pp. 238–240, 1984.
[17] F. Pardo *et al.*, "Experimental and theoretical study of ultrafast optical switching using guided mode excitation in silicon on sapphire," *IEEE J. Quant. Elect.*, vol. QE-23, pp. 545–550, 1987.
[18] J. J. Gerdes, "Bidirectional eigenmode propagation analysis of optical waveguides based on method of lines," *Elect. Lett.*, vol. 30, pp. 550–551, 1994.
[19] R. Pregla and T. Itoh, Ed., *Numerical Techniques for Microwave and Millimeter-Wave Passive Structures*. New York: Wiley, 1989.
[20] S. J. Al-Bader and H. A. Jamid, "Guided waves in nonlinear saturable self-focusing thin films," *IEEE J. Quant. Elect.*, vol. QE-23, pp. 1947–1955, 1987.
[21] M. Bertoletti, P. Masciulli, and C. Sibilia, "Mol numerical analysis of nonlinear planar waveguides," *IEEE J. Lightwave Technol.*, vol. 12, pp. 784–789, 1994.

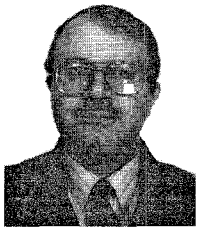

Samir J. Al-Bader received the B.Sc. degree in electrical engineering from the University of Wales in 1965 and the M.Sc. degree in electronics from the University of Bradford, U.K., in 1968. Between 1968 and 1971 he conducted research on microwaves at the University of Leeds, U.K., from which he received the degree of Ph.D. in 1971.

He is Professor of Electrical Engineering at the King Fahd University of Petroleum & Minerals, Dhahran, Saudi Arabia. He has been with the King Fahd University since 1972 where, along with teaching and research activities, he has chaired the Electrical Engineering Department from 1974 to 1978 and again from 1979 to 1980. He has undertaken sponsored research work on tropospheric wave propagation and has also been doing research into integrated optics with current interest in modeling linear and nonlinear guided wave devices.

Hussain A. Jamid was born in Qatif, Saudi Arabia on August 15, 1956. He received both the B.Sc. and M.Sc. degrees in electrical engineering from Arizona State University, Tempe, in 1981 and 1983, respectively. He received the Ph.D. degree from the King Fahd University of Petroleum and Minerals, Dhahran, Saudi Arabia in 1986.

He is currently Associate Professor of electrical engineering at the King Fahd University of Petroleum and Minerals. He took research leave with the University of Bath, U.K., from 1986 to 1987. His research interests are integrated optical guided waves and nonlinear integrated optics.